Inorganic Chemistry

Article

pubs.acs.org/IC

Non-Phase-Transition Luminescence Mechanochromism of a Copper(I) Coordination Polymer

Eunjin Kwon, Jineun Kim, Kang Yeol Lee,* and Tae Ho Kim*

Department of Chemistry (BK21 plus) and Research Institute of Natural Science, Gyeongsang National University, Jinju 52828, Korea

Supporting Information

ABSTRACT: A copper(I) coordination polymer, $[Cu_2I_2L_2]_n$ (CP **1**), shows luminescence mechanochromism with a color change from greenish-blue to yellow upon the application of pressure. Powder X-ray diffraction and Raman studies reveal that the changes in the bond lengths in crystalline CP **1** are the main cause of luminescence mechanochromism. The luminescence mechanochromic process of CP **1** preserves its crystallinity with a small lattice distortion, despite very high pressure, and it is a non-phase-transition process. After the addition of several drops of acetonitrile to the ground and compressed samples, the original greenish-blue emissive and crystalline states are restored. Therefore, the luminescence color conversion processes are fully reversible.

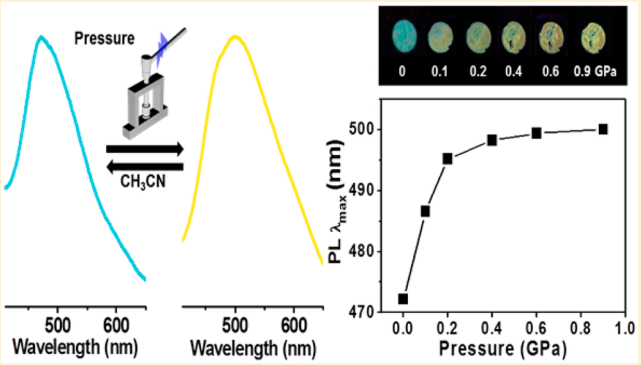

INTRODUCTION

Recently, research on novel functional coordination polymers (CPs) as stimuli-responsive intelligent materials with tunable photoluminescence (PL) has gained substantial momentum, because of their potential applications as sensors,[1] PL switches,[2] and optical recording devices.[3] An external stimuli-induced reversible color change is called chromism.[4] Several different types of chromisms, such as photochromism,[5] electrochromism,[6] thermochromism,[7] mechanochromism,[8] solvatochromism,[9] etc., have been defined and commonly reported. Among these, mechanochromism represents a color change initiated by mechanical stresses, such as grinding, compressing, shearing, and other external mechanical forces.

The phenomenon of luminescence mechanochromism, which is also known as mechanoluminescence, was first discovered by Francis Bacon.[10] Interestingly, mechanochromism is mostly accompanied by a phase transition such as a crystal-to-amorphous transition[11] and/or an aggregation state change.[12] Furthermore, design strategies for luminescence mechanochromism are few and an understanding of the underlying mechanism is still lacking. Although several structural factors, such as molecular arrangement, conformational flexibility, and intermolecular interactions, have been proposed to result in luminescence mechanochromism, its exact origin has remained unclear. The main reason behind the difficulty in identifying the origin of luminescence mechanochromism is the loss of crystallinity when emissive samples are mechanically compressed. A majority of the reports on this phenomenon are based on organic systems.[13] So far, complexes containing several metal ions[14] (Cu(I),[15] Zn(II),[16] Pt,[17] Ag,[18] and Au[19]) have been reported to show excellent luminescence mechanochromism. However, CPs with luminescence mechanochromic properties are still rarely studied, although mechanochemical processes have a long history.

In this work, our aim was to examine the reversibility of the luminescence mechanochromism of a new copper(I) CP under the application of a mechanical stress. To this end, we designed and synthesized an organic functional ligand 3-(2-(benzylthio)-ethoxy)pyridine (**L**) for the formation of a coordination polymer (CP **1**) with CuI. Herein, we show that the luminescence mechanochromism of CP **1** is caused by modification of the bond strengths accompanied by changes of the *d*-spacing distances of the specific lattice planes, which are also proved by the bathochromic shifts of Raman frequencies. Interestingly, the luminescence mechanochromism of CP **1** is a non-phase-transition process, despite the application of very high pressures (>0.1 GPa).

RESULTS AND DISCUSSION

An N/S donor ligand, **L**, was synthesized from 3-hydroxypyridine and benzyl 2-chloroethylsulfide via a previously reported method[20] (see Scheme S1 in the Supporting Information (SI)) since Cu_2I_2 complexes with aromatic N and S donor ligands show photoluminescence. In addition, a benzyl group was introduced for possible intermolecular $\pi-\pi$ interactions. The luminescent CP **1**, $[Cu_2I_2L_2]_n$, was prepared by the reaction between CuI and **L**, taken in a 1:1 molar ratio in acetonitrile. Figure 1 shows the single-crystal X-ray structure of CP **1**. The pale yellow crystalline CP **1** crystallizes with a monoclinic

Received: October 25, 2016

DOI: 10.1021/acs.inorgchem.6b02571
Inorg. Chem. XXXX, XXX, XXX−XXX

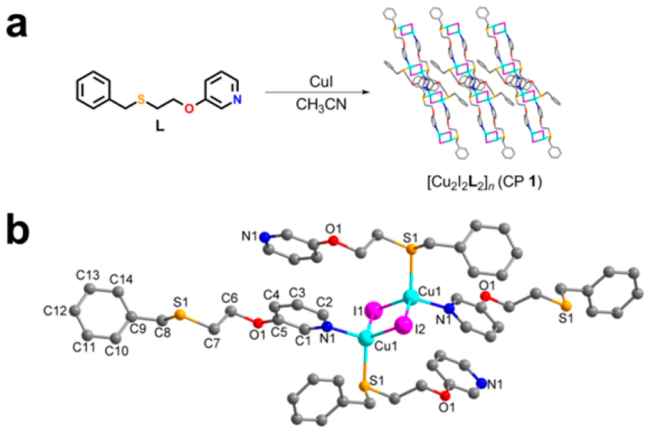

Figure 1. (a) Synthetic scheme of CP **1** and (b) its coordination environment. Hydrogen atoms are omitted for the sake of clarity.

crystal system, space group *C*2/*c* (Figure S1 in the SI). CP **1** shows a one-dimensional (1D) loop chain structure (Figure 1a, right).

Crystallographic data and bond lengths/angles for CP **1** are summarized in Table 1 and Table S2 in the SI. Figure 1b shows

Table 1. Crystallographic Data of CP 1

parameter	value
formula	$C_{14}H_{15}CuINOS$
formula weight	435.77
temperature	173(2) K
crystal system	monoclinic
space group	*C*2/*C*
a	14.9694(8) Å
b	17.0368(8) Å
c	11.7309(6) Å
β	92.621(2)°
V	2988.6(3) Å^3
Z	8
D_{calc}	1.937 g cm^{-3}
F(000)	1696
q range	1.812−27.607
reflections collected	13679
independent reflections	3441
R (int)	0.0281
goodness of fit, *F*2	1.037
R, $wR^2(I > 2\sigma(I))$	R_1 = 0.0273, wR_2 = 0.0708
R_1 and wR_2 indices (all data)[a]	R_1 = 0.0313, wR_2 = 0.0738

[a] $R_1 = \sum||F_o| - |F_c||/\sum|F_o|$. $\omega R_2 = \sum[w(F_o^2 - F_c^2)^2]/\sum[w(F_o^2)^2]^{1/2}$.

the coordination environment of CP **1**. The asymmetric unit of CP **1** consists of a Cu(I) ion, an μ_2-iodide, and a **L**. Cu(I) bonding with two iodides, a S atom, and a pyridyl N atom exhibits a distorted tetrahedral coordination geometry. A Cu_2I_2 rhomboid dimer is generated by an inversion symmetry operation of the asymmetric unit. The packing diagrams and intermolecular interactions of CP **1** are shown in Figure 2.

Each compartment of the loop chain contains one rhomboid dimer Cu_2I_2 cluster and two **L**. The Cu−Cu (2.9456(8) Å), Cu−S (2.3246(9) Å), Cu−I (2.6380(4)−2.6762(4) Å), and Cu−N (2.066(2) Å) distances are similar to those in Cu(I) complexes. In the crystal, C−H···O hydrogen bonds (C7···O1, 3.532(4) Å; H7B···O1, 2.56 Å) link adjacent molecules (see Figure 2). In addition, crystal packing is stabilized by weak

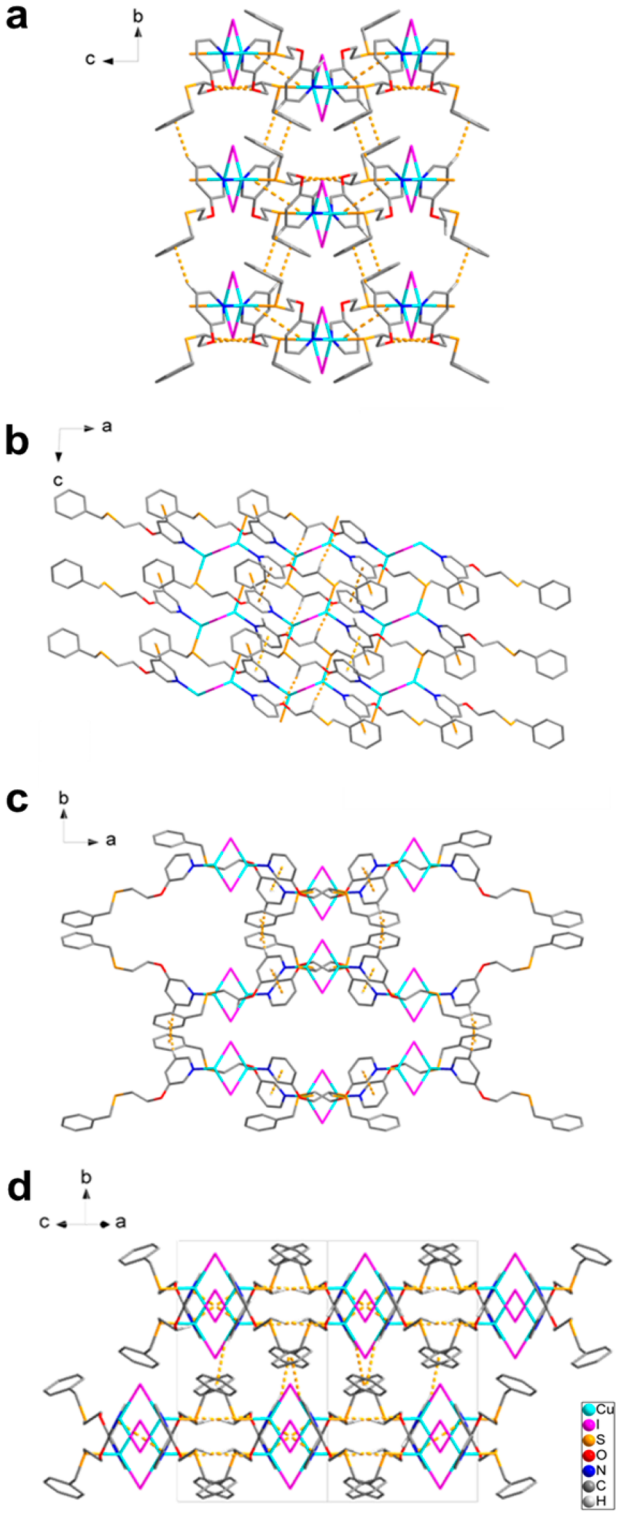

Figure 2. Packing diagrams of CP **1** along (a) the *a*-axis, (b) the *b*-axis, (c) the *c*-axis, and (d) the [101] direction.

intermolecular C−H···π (C3−H3···Cg_2 = 2.63 Å, where Cg_2 is the centroid of the C9−C14 ring) and π−π interactions ($Cg1$···$Cg1$ = 3.6546(17) Å, where $Cg1$ is the centroid of the ring formed by N1 and C1−C5 atoms) (see Figure 1b for labeling).

The loop chains are lined up along the [101] direction. The chains are linked by weak intermolecular C−H···π interactions (2.63 Å), resulting in a three-dimensional architecture.

DOI: 10.1021/acs.inorgchem.6b02571
Inorg. Chem. XXXX, XXX, XXX−XXX

Thermogravimetric analysis (TGA), shown in Figure 3, was conducted to investigate the thermal stability of CP **1**. The

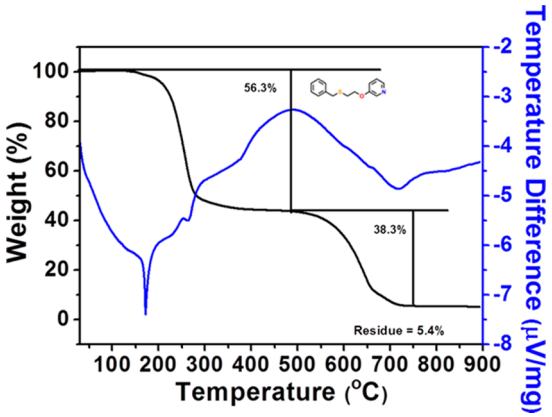

Figure 3. TGA (black) and DTA (blue) traces of CP **1**.

weight loss of CP **1** occurred in two distinct regions: the 147−487 °C range and the 487−780 °C range (black trace in Figure 3). The first weight loss (~56%) in the temperature range of 147−487 °C was induced by the decomposition of the ligand molecules in CP **1** crystals. This is in good agreement with the calculated value of 56.3%. The second weight loss originated from the decomposition of the residual compound left behind from the first step, leaving ~5% residue.

The differential thermal analysis (DTA) data (black trace in Figure 3) was also acquired during the TGA measurements; these results indicated a remarkable endothermic reaction at 175 °C, which was assigned to the decomposition of the organic ligands in CP **1** (blue trace in Figure 3). We believe that the endothermicity of the peak in the DTA trace is caused by breaking of the covalent coordination bonds, and the corresponding weight loss is due to the low thermal stability of the bond between Cu and S atoms.[21]

Cu_xI_x cluster compounds have been studied by many research groups in regard to their photophysical properties such as luminescence thermochromism,[22] luminescence vapochromism,[23] and luminescence mechanochromism.[24] PL in Cu(I) CPs with N/S or N/P donor ligands and various Cu_xI_x geometries such as rhomboid-like,[25] stair step-like,[26,27] cubane-like,[27] etc. is a phenomenon observed in many cases. CP **1** radiates a greenish-blue light upon ultraviolet (UV) irradiation (356 nm).

The PL color of CP **1** changed from greenish-blue to yellow after grinding in a mortar (Figure S2a in the SI). Overall, the crystallinity of CP **1** was preserved, despite the strenuous grinding (Figure S2b). Interestingly, the powder X-ray diffraction (PXRD) patterns (Figure S2a) of CP **1** before and after grinding indicate that CP **1** did not undergo any phase transition, such as crystal-to-amorphous conversion, even though the PL color changed from greenish-blue to yellow. Based on the above observations, the crystal structure of CP **1** is expected to sustain even high pressures. Therefore, a high pressure (0.1−0.9 GPa) was gradually applied on CP **1** crystals in order to observe any change in its crystallinity and PL spectra.

Figure 4a shows the spectral shift of the PL band of polycrystalline CP **1** after compression. It can be easily noticed from the figure that increasing the pressure from 0 to 0.9 GPa leads to a gradual bathochromic shift of the PL band of CP **1**

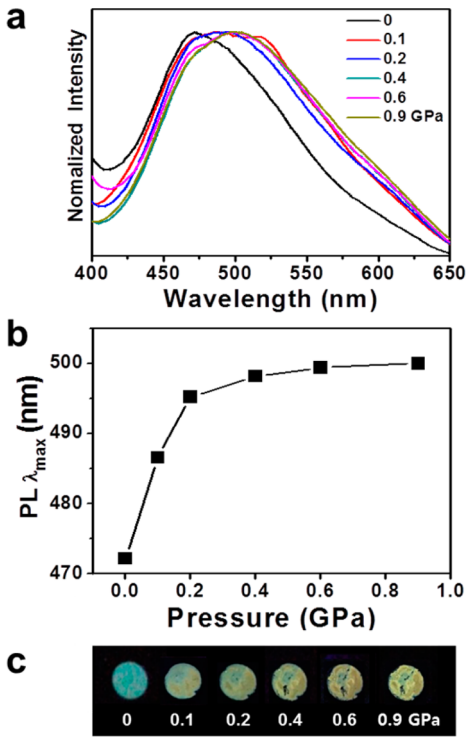

Figure 4. (a) Variation of PL spectra of the solid-state CP **1** coordination polymers with pressure. (b) Variation of emission maximum with pressure, showing a plateau after ~0.4 GPa. (c) Photographic images of compressed CP **1** pellets under UV irradiation; the dark spots in the compressed sample disks are due to small defects.

from 472 nm to 500 nm. The PL maximum plateaus after 0.4 GPa (Figure 4b). The spectral shift was also accompanied by a distinct color change from greenish-blue to yellow (Figure 4c). The above-mentioned bathochromic shift of the PL peak induced by mechanical pressure, which is the so-called "luminescence mechanochromism", can be reasonably explained in terms of the release of internal energy by the crystalline CP **1**. Generally, when work is done on a crystal via coercive compression, the internal energy in an adiabatic process increases. In the case of CP **1**, positions of the molecular orbitals will probably rearrange for compensating the increased internal energy caused by the applied high pressure. In particular, the energy gap between the highest occupied molecular orbital (HOMO) and lowest unoccupied molecular orbital (LUMO) of CP **1** must be reduced in order to explain the bathochromic shift.

Therefore, the emission energy by the metal-to-ligand charge transfer (MLCT) and halide-to-metal charge transfer (XMCT) will decrease with increasing pressure. In our case, however, the PL maximum reaches a plateau after 0.4 GPa. This implies that consumption of the increase in internal energy with increasing applied pressure is limited.

The lattice parameters or the *d*-spacing distances of specific lattice planes are also expected to change in the compressed CP **1** crystals. Variation of the lattice parameters of CP **1** with pressure were further confirmed by systematically investigating the PXRD patterns before and after compression (Figure 5), in comparison with the single-crystal X-ray diffraction (SCXRD) data at atmospheric pressure (Figure S2 in the SI). It can be seen that no new diffraction peak(s) appeared after the compression process, implying that no new crystalline phase

DOI: 10.1021/acs.inorgchem.6b02571
Inorg. Chem. XXXX, XXX, XXX−XXX

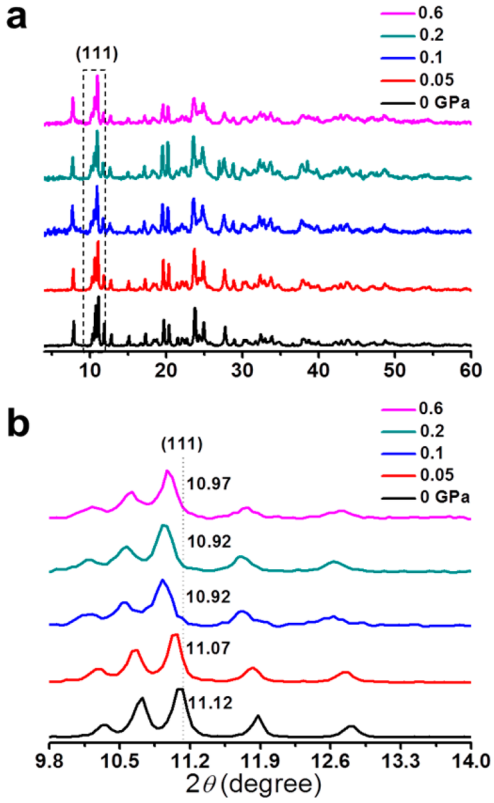

Figure 5. (a) PXRD patterns of CP **1** crystals before compression (black trace) and after compression (0.1 GPa, red trace; 0.1 GPa blue trace; 0.2 GPa green trace; 0.6 GPa pink trace). (b) Magnified PXRD patterns of the region depicted by dashed lines in panel (a).

was formed. Each PXRD pattern exhibits several diffraction peaks in the range of $4° < 2\theta < 60°$, which indicates that the crystallinity was preserved, despite the formation of the many defects induced by the high pressure. For further detailed PXRD analyses, the dashed region of the PXRD patterns in the range of $9.8° < 2\theta < 14°$ in Figure 5a were magnified in Figure 5b. When pressure is increased, a (111) major peak is shifted to smaller 2θ values (Figure 5b).

$$d = \frac{\lambda}{2 \sin \theta} \quad (1)$$

The d-spacing value of the (111) lattice plane in CP **1** crystal can be determined by eq 1.[28] The d-spacing of the (111) plane was 7.96, 7.99, and 8.09 Å at 0, 0.05, and 0.4 GPa, respectively. Interestingly, the d-spacing value of the (111) plane of the sample compressed with 0.4 GPa is ~0.13 Å and longer than that of CP **1** at 1 atm (see Figure S3 in the Supporting Information). As mentioned earlier, when work is done on a crystal by coercive compression, the internal energy in an adiabatic process will increase. Generally, under this condition, the d-spacing of the crystal plane under high pressure should be shorter than that of the crystal plane at normal pressure. However, in this study, the d-spacing of the crystal plane of CP **1** increased with applied high pressure, because the internal energy accumulated during compression was released by the change of the packing state of the lattice. Presumably, if the pressure acts on the samples in the side or vertical direction of the single crystal structure, as shown in Figure S3, the d-spacing value will increase and the chains of CP **1** will be elongated, resulting in longer bond distances. This can be validated by appearance of vibrational frequencies at lower values in the Raman spectra of the compressed samples.

To validate the change of the coordination environment around the $[Cu_2I_2]$ core (i.e., an increase in bond distances by applied pressure), Raman spectroscopy was performed and the spectra are shown in Figure 6. Raman spectra of solid CP **1** and compressed samples of CP **1** (0.1 and 0.6 GPa) were obtained with an excitation wavelength of 785 nm (Figure 6a). The black

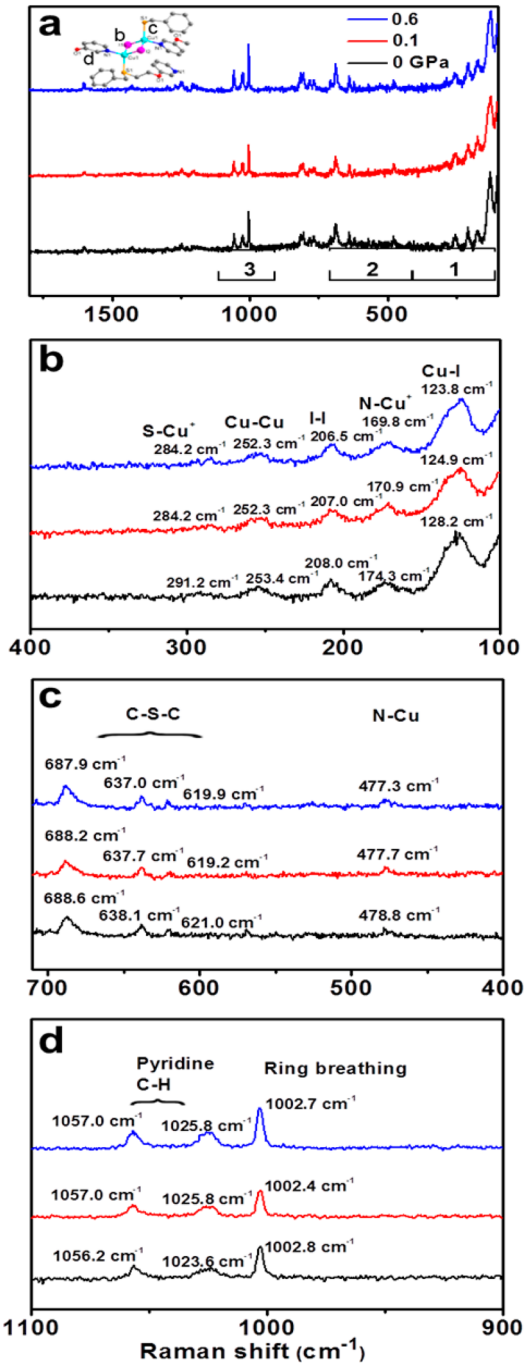

Figure 6. (a) Raman spectra of uncompressed CP **1** (black trace) and compressed CP **1** (0.1 GPa, red trace; 0.6 GPa, blue trace) obtained using excitation wavelength of 785 nm. (b) Magnified Raman spectra of the underlined region 1 shown in panel (a). (c) Magnified Raman spectra of the underlined region 2 shown in panel (a). (d) Magnified Raman spectra of the underlined region 3 shown in panel (a).

DOI: 10.1021/acs.inorgchem.6b02571
Inorg. Chem. XXXX, XXX, XXX−XXX

trace in Figure 6 shows the Raman spectrum obtained with CP **1**. The Raman spectra exhibited ~10 major vibrational peaks. The observed peaks at 128.2, 208.0, 253.4, 291.2, 478.8, (621.0, 638.1, 688.6), 1002.8, and (1023.6 and 1056.6) cm^{-1} can be assigned to the Cu−I stretching,[29] N−Cu stretching,[30] I−I stretching,[31] Cu−Cu stretching,[30] S−Cu,[30] N−Cu stretching,[32] S−C stretching (~620−689 cm^{-1}),[33] ring breathing (pyridine),[34] and C−H in plane bending[34] (1023.6 and 1056.6 cm^{-1}), respectively. Under high pressure, neither any Raman peaks disappeared nor any new Raman peaks were observed, indicating that the luminescence mechanochromic process in CP **1** is not accompanied by a phase change, as inferred from the PXRD patterns.

Generally, it is known that stretching and bending vibration modes adequately reflect bond lengths and bond angles. Modification of the coordination bond strengths (i.e., the peak shifts for each vibration mode), because of the applied pressure, can also influence the bathochromic shift of the MLCT or XLCT.[35] In Figure 6a, the red and blue traces display the spectral data of CP **1** compressed by a pressure of 0.1 and 0.6 GPa, respectively.

The original backbone structure is retained in the compressed CP **1** samples (Figure 6a), since their Raman spectra show the same peaks as the uncompressed CP **1**. However, the Raman peaks for the compressed CP **1** occur at lower frequencies (0.5−2 cm^{-1}). Except for the ring breathing and in-plane bending modes, the peaks corresponding to Cu−I, N−Cu, I−I, and Cu−Cu vibrations shift from 128.2, 174.3, 208.0, and 253.4 cm^{-1} to 123.8, 169.8, 206.5, and 252.3 cm^{-1}, respectively. This is in good agreement with elongation of the bonds around the coordination sphere, which is consistent with longer *d*-spacing distances induced by pressure. This elongation of the coordination covalent bonds raises the energy levels of the bonding orbitals between Cu(I) and ligands and lowers those of the antibonding orbitals (^{1}(M+X)LCT or ^{3}(M+X)LCT levels).

Therefore, the energy difference between the antibonding orbitals and HOMO becomes smaller, resulting in a bathochromic shift. Systematic correlation of the pressure-induced data obtained thus far can be summarized as follows. The solid-state emission, PXRD, and Raman studies show that the internal energy consumption and bond length (between the metal cation and organic ligand) variation by applied high pressure in the crystalline state are the main causes of the luminescence mechanochromism of CP **1**.

Interestingly, CP **1** also exhibits solvatochromic behavior with the color changing from yellow to greenish-blue by adding a few drops of acetonitrile solvent on the ground and compressed CP **1** samples, as shown in Figure 7 and Figure S4 in the SI, respectively.

Thus, the PL property of CP **1** was reversibly controlled by applying pressure and adding an organic solvent.[36] The change of PL by addition of acetonitrile may be understood in terms of the restoration of any defects or squeezed internal spaces and of the coordination environment of Cu_2I_2 cores in the compressed crystals to their original states within 1 min of adding a few drops of acetonitrile. We found that this process could be repeated for several cycles without any decomposition. To the best of our knowledge, this is the first report of luminescence mechanochromism exhibited by Cu(I) complexes comprising of a rhomboid Cu−I_2−Cu unit.

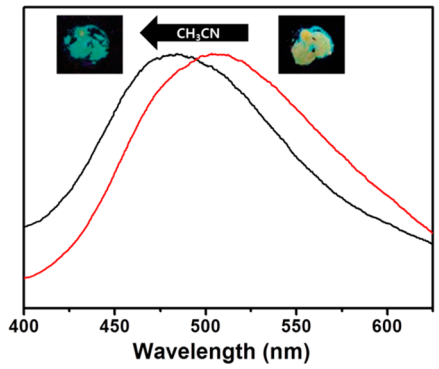

Figure 7. Photoluminescence spectra of CP **1** before (red curve) and after (black curve) the addition of acetonitrile on the compressed sample (0.6 GPa).

CONCLUSION

We designed and synthesized a bidentate ligand, 3-(2-(benzylthio)ethoxy)pyridine (**L**). A Cu(I) coordination polymer (CP **1**) was successfully synthesized by a self-assembly reaction between CuI and **L** and characterized by thermogravimetric analysis (TGA), photoluminescence (PL), and powder X-ray diffraction (PXRD). CP **1** was determined to have a one-dimensional loop-chain structure comprising of rhomboid Cu−I_2−Cu units interconnected by **L**. The luminescence mechanochromism of CP **1** involving a color change from greenish-blue to yellow was induced by applying pressure (0.1−0.9 GPa), while the crystallinity was preserved in the compressed CP **1** samples. The luminescent mechanochromism of CP **1** was a non-phase-transition process, despite very high applied pressures, as evidenced by PXRD patterns of the compressed samples. After the addition of several drops of acetonitrile to the ground samples (shown in Figure S4 in the SI) and compressed samples (see Figure 7), the emission color was reverted to the original greenish-blue and also the samples themselves were restored to the original state of CP **1**.

We also showed that the coordination environment around the Cu cation can be easily perturbed by physical pressure (0.1−0.9 GPa) to change the PL property. Both the *d*-spacing distance calculation and Raman frequency shifts strongly supported that external mechanical force can have a significant influence on the bond distances in the solid state. CP **1** exhibited luminescence mechanochromic behavior with a color contrast between greenish-blue and yellow. The solid-state emission, PXRD and Raman studies reveal that the internal energy consumption and bond length variations between metal cation and **L** induced by the applied high pressures in the crystalline state are the main cause of the luminescence mechanochromism of CP **1**.

This high-pressure-induced phenomenon not only suggests a novel field for luminescence mechanochromic materials, but also motivates and accelerates further development of CP-based pressure sensors. In addition to providing a fundamental understanding of their properties, this study demonstrates their potential for applications in sensing and detection devices. Finding recoverable mechanochromic materials with a fast response remains a challenge for their potential applications. The development of stimuli responsive materials based on these copper(I) clusters is currently under investigation.

DOI: 10.1021/acs.inorgchem.6b02571
Inorg. Chem. XXXX, XXX, XXX−XXX

EXPERIMENTAL SECTION

Chemicals. 2-Bromoethanol (C_2H_5BrO, ≥95.0%, 124.97 g/mol) was purchased from TCI. Thionyl chloride ($SOCl_2$, ≥99%, 118.97 g/mol), benzyl mercaptan (C_7H_8S, 99%, 124.2 g/mol) and 3-hydroxypyridine (C_5H_5NO, 98%, 95.10 g/mol) were purchased from Sigma–Aldrich. Potassium hydroxide (KOH, 56.11 g/mol) was purchased from Daejung Chemicals. All reagents were used as received without further purification.

Synthesis of 3-(2-(Benzylthio)ethoxy)pyridine (L). Benzyl mercaptan (6.8 g, 55 mmol) was added to 2-bromoethanol (6.8 g, 55 mmol) in the presence of potassium hydroxide (3.1 g, 55 mmol) in tetrahydrofuran (THF). The mixture was refluxed for 3 h and cooled to room temperature, at which point it was back-extracted with THF. The combined organic layers, dried with anhydrous sodium sulfate, were evaporated. Thionyl chloride (4.0 mL, 55 mmol) in chloroform then was added to the resulting solution. The solution was refluxed and stirred for 1 h. After being sufficiently cooled, it was then placed into a small amount of methanol, followed by stirring for 1 h to decompose the excess of thionyl chloride. The mixture was added to 3-hydroxypyridine (5.2 g, 55 mmol) in the presence of potassium hydroxide (3.1 g, 55 mmol) in THF. The mixture was refluxed for 24 h and cooled to room temperature. An organic layer was collected and a water layer was extracted with dichloromethane. The combined organic layers dried with anhydrous sodium sulfate were evaporated. Column chromatography (silica gel, ethyl acetate/*n*-hexane = 40/60 (v/v), R_f = 0.33) gave a pure product (8.3 g, 62%). ^{1}H NMR (300 MHz, $CDCl_3$): δ = 8.16 (d, 2H, Py), 7.22 (t, 2H, Py), 7.19 (m, 5H, Ph), 3.94 (t, 2H, OCH_2), 3.69 (s, 2H, SCH_2Ph), 2.68 (t, 2H, CH_2S). ^{13}C NMR (75.4 MHz, $CDCl_3$): δ = 156.66, 142.31, 138.096, 137.98, 128.94, 128.86, 128.62, 127.23, 123.88, 121.11, (solvent: 77.72, 77.30, 76.87), 67.93, 36.79, 29.99. IR (KBr, ν, cm^{-1}): 3060 s, 3029 s, 2923 s, 2502 m, 1702 m, 1576 s, 1476 s, 1460 s, 1426 s, 1264 s, 1231 s, 1204 m, 1130 m, 1049 s, 1009 s, 801 s, 768 s, 702 s, 621 m, 565 m, 474 m, 415 m. Mass spectrum *m*/*z* 245 (M^+).

Synthesis of $[Cu_2I_2L_2]_n$ (1). **L** (0.012 g, 0.05 mmol) and CuI (0.010 g, 0.05 mmol) was allowed to mix in an acetonitrile (1 mL) solvent. Pale yellow precipitates were filtered and washed with diethyl ether/acetonitrile (2/1) solution (0.033 g, 66%). IR (KBr, ν, cm^{-1}): 3060 w, 3029 w, 2913 w, 1574 s, 1475 s, 1460 m, 1426 s, 1266 s, 1227 s, 1202 m, 1140 m, 1055 m, 995 s, 802 m, 779 m, 700 s, 637 w, 567 w, 480 w, 418 w. $[CuIL]_n$ Anal. Calcd for $C_{14}H_{15}CuINOS$: C 38.59, H 3.47, N 3.21, S 7.36. Found: C 38.42, H 3.37, N 3.60, S 7.23%.

Characterization. The powder X-ray diffraction (PXRD) patterns were obtained with a diffractometer (Bruker, Model AXS D8 Advance), using Cu Kα (1.54056 Å) radiation. The ^{1}H and ^{13}C NMR spectra were recorded on an NMR spectrometer (Bruker, Model Avance-300 (300 MHz)). The IR spectra were obtained within the 4000–400 cm^{-1} as KBr disks on a spectrometer (Varian, Model 640-IR). Raman spectra were obtained using a spectrometer (Horiba Jobin Yvon/LabRAM, Model ARAMIS IR2) with a 785 nm line for a diode laser as an excitation source. Elemental analysis (EA) was performed on a PerkinElmer Model 2400 analyzer. Thermogravimetric analysis (TGA) and differential thermal analysis (DTA) were performed under nitrogen at a scan rate of 10 °C min^{-1}, using a thermogravimetric analyzer (TA Instruments, Model SDT Q600). ESI-mass spectra were obtained on a Thermo Scientific LCQ spectrometer. Solid-state luminescence spectra were recorded on a spectrophotometer (Hitachi, Model F-7000).

Crystallographic Details. Single-crystal diffraction data for CP **1** were also collected with a Bruker SMART APEX II ULTRA diffractometer. The cell parameters for the compounds were obtained from a least-squares refinement of the spots (from 36 collected frames). Data collection, data reduction, and semiempirical absorption correction were carried out using APEX2.[37] All of the calculations for the structure determination were carried out using SHELXTL.[38] In all cases, all nonhydrogen atoms were refined anisotropically and all hydrogen atoms were placed in calculated positions and refined isotropically in a riding manner, along with their respective parent atoms.

Solid-State Luminescence Spectra Measurement. Solid-state luminescence spectra were recorded with powder and pellet samples on a Shimadzu Model JP/SSP-10A system at room temperature. The pellet samples were prepared by applying pressures of 0.1–0.9 GPa at a constant time of 10 s after putting the powder into the KBr pellet making device (hand press).

ASSOCIATED CONTENT

Supporting Information

The Supporting Information is available free of charge on the ACS Publications website at DOI: 10.1021/acs.inorgchem.6b02571.

Experimental details for the synthesis of ligand **L**; PXRD patterns and photoluminescence spectra of a ground sample; copies of the data CCDC 1505970 can be obtained free of charge from the Cambridge Crystallographic Data Centre via http://www.ccdc.cam.ac.uk/data_request/cif(PDF)
(CIF)

AUTHOR INFORMATION

Corresponding Authors

*E-mail: k9876047266@gmail.com.
*E-mail: thkim@gnu.ac.kr.

ORCID

Kang Yeol Lee: 0000-0001-8055-1635
Tae Ho Kim: 0000-0003-0415-7374

Notes

The authors declare no competing financial interest.

ACKNOWLEDGMENTS

This research was supported by the Basic Science Research Program through the National Research Foundation of Korea (NRF) funded by the Ministry of Education, Science and Technology (Nos. 2014R1A1A4A01009105, 2015R1D1A4A01020317, and 2016R1D1A3B03934096).

REFERENCES

(1) Chen, J.; Yi, F.-Y.; Yu, H.; Jiao, S.; Pang, G.; Sun, Z.-M. Fast Response and Highly Selective Sensing of Amine Vapors Using a Luminescent Coordination Polymer. *Chem. Commun.* **2014**, *50*, 10506–10509.

(2) Tong, J.; Wang, Y.; Mei, J.; Wang, J.; Qin, A.; Sun, J. Z.; Tang, B. Z. A 1,3-Indandione-Functionalized Tetraphenylethene: Aggregation-Induced Emission, Solvatochromism, Mechanochromism, and Potential Application as a Multiresponsive Fluorescent Probe. *Chem.—Eur. J.* **2014**, *20*, 4661–4670.

(3) Czerwinski, F.; Zielinska-Lipiec, A.; Szpunar, J. A. Thermal Instability of Ni Electrodeposits Applied in Replication of Optical Recording Devices. *Acta Mater.* **1999**, *47*, 2553–2566.

(4) Sheth, A. R.; Lubach, J. W.; Munson, E. J.; Muller, F. X.; Grant, D. J. W. Mechanochromism of Piroxicam Accompanied by Intermolecular Proton Transfer Probed by Spectroscopic Methods and Solid-Phase Changes. *J. Am. Chem. Soc.* **2005**, *127*, 6641–6651.

(5) Browne, W. R.; Pollard, M. M.; de Lange, B.; Meetsma, A.; Feringa, B. L. Reversible Three-State Switching of Luminescence: A New Twist to Electroand Photochromic Behavior. *J. Am. Chem. Soc.* **2006**, *128*, 12412–12413.

(6) Maier, A.; Cheng, K.; Savych, J.; Tieke, B. Double-Electrochromic Coordination Polymer Network Films. *ACS Appl. Mater. Interfaces* **2011**, *3*, 2710–2718.

(7) Yan, Z.-H.; Li, X.-Y.; Liu, L.-W.; Yu, S.-Q.; Wang, X.-P.; Sun, D. Single-Crystal to Single-Crystal Phase Transition and Segmented

DOI: 10.1021/acs.inorgchem.6b02571
Inorg. Chem. XXXX, XXX, XXX–XXX

Thermochromic Luminescence in a Dynamic 3D Interpenetrated Ag^{I} Coordination Network. *Inorg. Chem.* **2016**, *55*, 1096−1101.
(8) Benito, Q.; Baptiste, B.; Polian, A.; Delbes, L.; Martinelli, L.; Gacoin, T.; Boilot, J.-P.; Perruchas, S. Pressure Control of Cuprophilic Interactions in a Luminescent Mechanochromic Copper Cluster. *Inorg. Chem.* **2015**, *54*, 9821−9825.
(9) Park, G.; Yang, H.; Kim, T. H.; Kim, J. Copper(I) Coordination Polymers of *N,N′*-Bis[3-(methylthio)propyl]pyromellitic Diimide: Crystal Transformation and Solvatochromism by Halogen−π Interactions. *Inorg. Chem.* **2011**, *50*, 961−968.
(10) Eddingsaas, N. C.; Suslick, K. S. Intense Mechanoluminescence and Gas Phase Reactions from the Sonication of an Organic Slurry. *J. Am. Chem. Soc.* **2007**, *129*, 6718−6719.
(11) Qi, Q.; Zhang, J.; Xu, B.; Li, B.; Zhang, S. X-A.; Tian, W. Mechanochromism and Polymorphism-Dependent Emission of Tetrakis(4-(dimethylamino)phenyl)ethylene. *J. Phys. Chem. C* **2013**, *117*, 24997−25003.
(12) Chan, C. Y. K.; Lam, J. W. Y.; Zhao, Z.; Chen, S.; Lu, P.; Sung, H. H. Y.; Kwok, H. S.; Ma, Y.; Williams, I. D.; Tang, B. Z. Aggregation-Induced Emission, Mechanochromism and Blue Electroluminescence of Carbazole and Triphenylamine-Substituted Ethenes. *J. Mater. Chem. C* **2014**, *2*, 4320−4327.
(13) Chi, Z.; Zhang, X.; Xu, B.; Zhou, X.; Ma, C.; Zhang, Y.; Liu, S.; Xu, J. Recent Advances in Organic Mechanofluorochromic Materials. *Chem. Soc. Rev.* **2012**, *41*, 3878−3896.
(14) Zhang, X.; Chi, Z.; Zhang, Y.; Liu, S.; Xu, J. Recent Advances in Mechanochromic Luminescent Metal Complexes. *J. Mater. Chem. C* **2013**, *1*, 3376−3390.
(15) Benito, Q.; Le Goff, X. F. L.; Maron, S.; Fargues, A.; Garcia, A.; Martineau, C.; Taulelle, F.; Kahlal, S.; Gacoin, T.; Boilot, J.-P.; Perruchas, S. Polymorphic Copper Iodide Clusters: Insights into the Mechanochromic Luminescence Properties. *J. Am. Chem. Soc.* **2014**, *136*, 11311−11320.
(16) Tzeng, B.-C.; Chang, T.-Y.; Sheu, H.-S. Reversible Phase Transformation and Luminescent Mechanochromism of Zn^{II}-Based Coordination Frameworks Containing a Dipyridylamide Ligand. *Chem.—Eur. J.* **2010**, *16*, 9990−9993.
(17) Krikorian, M.; Liu, S.; Swager, T. M. Columnar Liquid Crystallinity and Mechanochromism in Cationic Platinum(II) Complexes. *J. Am. Chem. Soc.* **2014**, *136*, 2952−2955.
(18) Liu, L.; Wen, T.; Fu, W.-Q.; Liu, M.; Chen, S.; Zhang, J. Structure-Dependent Mechanochromism of Two Ag(I) Imidazolate Chains. *CrystEngComm* **2016**, *18*, 218−221.
(19) Seki, T.; Takamatsu, Y.; Ito, H. A Screening Approach for the Discovery of Mechanochromic Gold(I) Isocyanide Complexes with Crystal-to-Crystal Phase Transitions. *J. Am. Chem. Soc.* **2016**, *138*, 6252−6260.
(20) Kim, T. H.; Shin, Y. W.; Lee, S. S.; Kim, J. Supramolecular Assembly of One-Dimensional Channels and Two-Dimensional Brick-Wall Networks from Asymmetric Dithioether Ligands and Copper(I) Iodide. *Inorg. Chem. Commun.* **2007**, *10*, 11−14.
(21) Park, H.; Kwon, E.; Kang, G.; Kim, J.; Kim, T. H. Photoluminescent Copper(I) Complex Based on 3-(2-(Cyclohexylthio)ethoxy)pyridine: Synthesis, Structure, and Physical Properties. *Bull. Korean Chem. Soc.* **2016**, *37*, 1163−1165.
(22) Sun, D.; Yuan, S.; Wang, H.; Lu, H.-F.; Feng, S.-Y.; Sun, D.-F. Luminescence Thermochromism of Two Entangled Copper-Iodide Networks with a Large Temperature-Dependent Emission Shift. *Chem. Commun.* **2013**, *49*, 6152−6154.
(23) Kang, G.; Jeon, Y.; Lee, K. Y.; Kim, J.; Kim, T. H. Reversible Luminescence Vapochromism and Crystal-to-Amorphous-to-Crystal Transformations of Pseudopolymorphic Cu(I) Coordination Polymers. *Cryst. Growth Des.* **2015**, *15*, 5183−5187.
(24) Benito, Q.; Maurin, I.; Cheisson, T.; Nocton, G.; Fargues, A.; Garcia, A.; Martineau, C.; Gacoin, T.; Boilot, J.-P.; Perruchas, S. Mechanochromic Luminescence of Copper Iodide Clusters. *Chem.—Eur. J.* **2015**, *21*, 5892−5897.
(25) Jeon, Y.; Cheon, S.; Cho, S.; Lee, K. Y.; Kim, T. H.; Kim, J. Controlled Reversible Crystal Transformation of Cu(I) Supramolecular Isomers. *Cryst. Growth Des.* **2014**, *14*, 2105−21091.
(26) Kim, T. H.; Lee, S.; Jeon, Y.; Shin, Y. W.; Kim, J. Reversible Photoluminescence Switch: A Stair-Step Cu_4I_4 Coordination Polymer Based on a Dithioether Ligand. *Inorg. Chem. Commun.* **2013**, *33*, 114−117.
(27) Cho, S.; Jeon, Y.; Lee, S.; Kim, J.; Kim, T. H. Reversible Transformation between Cubane and Stairstep Cu_4I_4 Clusters Using Heat or Solvent Vapor. *Chem. - Eur. J.* **2015**, *21*, 1439−1443.
(28) Chang, Y.; Wang, H.; Zhu, Q.; Luo, P.; Dong, S. Theoretical Calculation and Analysis of ZrO_2 Spherical Nanometer Powders. *J. Adv. Ceram.* **2013**, *2*, 21−25.
(29) Socrates, G. *Infrared and Raman Characterisic Group Frequencies Tables and Charts*, 3rd Edition; John Wiley & Sons, Ltd: Chichester, U.K., 2001.
(30) Wallace-Williams, S. E.; James, C. A.; de Vries, S.; Saraste, M.; Lappalainen, P.; van der Oost, J.; Fabian, M.; Palmer, G.; Woodruff, W. H. Far-Red Resonance Raman Study of Copper A in Subunit II of Cytochrome *c* Oxidase. *J. Am. Chem. Soc.* **1996**, *118*, 3986−3987.
(31) Tveter, T.; Klaeboe, P.; Nielsen, C. J. Vibrational Spectra of the Charge Transfer Complexes between Organic Sulfides and Iodine. *Spectrochim. Acta, Part A* **1984**, *40*, 351−359.
(32) Baran, E. J.; Wagner, C. C.; Torre, M. H. Synthesis and Characterization of EDTA Complexes Useful for Trace Elements Supplementation. *J. Braz. Chem. Soc.* **2002**, *13*, 576−582.
(33) Upadhyay, G.; Gomti Devi, Th. Raman Bandshape Snalysis on C-H and CSC Stretching Modes of Dimethyl Sulfoxide in Liquid Binary Mixture: Comparative Study with Quantum-Chemical Calculations. *Spectrochim. Acta, Part A* **2014**, *133*, 250−258.
(34) Do, W. H.; Lee, C. J.; Kim, D. Y.; Jung, M. J. Adsorption of 2-Mercaptopyridine and 4-Mercaptopyridine on a Silver Surfaces Investigated by SERS Spectroscopy. *J. Ind. Eng. Chem.* **2012**, *18*, 2141−2146.
(35) Araki, H.; Tsuge, K.; Sasaki, Y.; Ishizaka, S.; Kitamura, N. Luminescence Ranging from Red to Blue: A Series of Copper(I)−Halide Complexes Having Rhombic $\{Cu_2(\mu\text{-}X)_2\}$ (X = Br and I) Units with *N*-Heteroaromatic Ligands. *Inorg. Chem.* **2005**, *44*, 9667−9675.
(36) Wang, Y.; Li, M.; Zhang, Y.; Yang, J.; Zhu, S.; Sheng, L.; Wang, X.; Yang, B.; Zhang, S. X-A. Stress Acidulated Amphoteric Molecules and Mechanochromism via Reversible Intermolecular Proton Transfer. *Chem. Commun.* **2013**, *49*, 6587−6589.
(37) *APEX2 Version 2014.11-0 Data Collection and Processing Software*; Bruker AXS, Inc.: Madison, WI, 2014.
(38) *SHELXTL-PC Version 6.22: Program for Solution and Refinement of Crystal Structures*; Bruker AXS, Inc.: Madison, WI, 2001.

DOI: 10.1021/acs.inorgchem.6b02571
Inorg. Chem. XXXX, XXX, XXX−XXX